

PHASE-FREE ACCELERATION OF CHARGED PARTICLES USING RECTANGULAR DRIFT TUBE-LOADED CAVITIES

W. Schott, H. Zinner, W. Wilhelm, H. Hagn and H. Daniel

Physik-Department der Technischen Universität München, Munich, Germany

Summary. Rectangular drift tube-loaded cavity resonators which were operated in the TE 101 mode have been tested for their use in a phase-free accelerator. Perturbing object measurements combined with numerical calculations show that the energy gain depends strongly on the shape of the drift tubes and on the position of the beams in the reference plane. Particles are accelerated in one direction within a range of about 10 cm using 25 cm wide drift tubes with straight and pointed shapes, respectively.

The energy gain of one cavity has been measured directly at an electromagnetic field amplitude of 1.6 Gauss and an electron beam of 20 keV. The time averaged energy gain of 15 eV is in good agreement with the theory.

An example of an accelerating device which might be used to produce a large circulating current of electrons of 50 MeV is sketched. The cavities are placed within the gaps of spiral ridge magnets.

Introduction

The phase-free acceleration of charged particles by means of two orthogonal electric and magnetic ac fields has been described in a preceding paper¹. In this paper a realization of the suggested method with rectangular drift tube-loaded cavity resonators which are operated in the TE 101 mode was outlined. An accelerating stage consists of four cavities whose phases are chosen in such a way that the particles enter the fields at phases differing by π , π , and 0 compared to the phase of the first cavity.

By insertion of a drift tube into a cavity the field distribution is disturbed. Thereby, the energy gain is changed. In order to check the influence of the drift tube shape on the energy gain, perturbing object measurements were performed. The measurements yield the field components. The energy gain is computed numerically using the measured data. The cavity and the drift tubes must be made flat in x-direction and wide in y-direction (cf. fig. 1) in order that the resonator can be placed within the gap of an FFAG guide field magnet permitting a rather small gap of the magnet and providing a large radial width for the reference orbits.

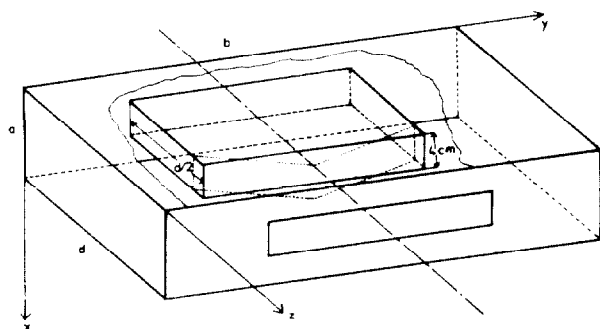


Fig. 1. Scheme of the cavity resonator which is operated in the TE 101 mode. $a = 0.100$, $b = 0.486$, $d = 0.208$ m. A rectangular and a pointed drift tube are sketched (full and dotted lines for the visible edges, respectively).

Energy gain values which were obtained by numerical calculations using the data of perturbing object measurements were compared with direct energy gain measurements of electrons after having passed one cavity, thus showing the validity of the perturbing object measurements.

Phase-free acceleration suggests to be a method for accumulating a large continuous current of relativistic electrons because it permits energy to be transferred into a continuous beam. The conditions for producing a large current of relativistic electrons should be met in a cyclic device with a spiral ridge magnetic guide field. Such an accelerator is sketched in the last section.

Theory of phase-free acceleration by ideal fields

In an ideal rectangular cavity which resonates in the TE 101 mode, only the field components E_y and B_x exist in the plane $x = a/2$ (cf. fig. 1). If it is assumed that the fields in the first halves of the cavities are perfectly shielded, the energy gain $(\Delta E)_1$ and $(\Delta E)_2$ of particles with rest mass m and charge e after having passed one cavity and an accelerating stage are respectively given by²

$$(\Delta E)_1 = \frac{e^2 B_0^2 a^2 c B}{4 \pi d m \gamma} \left[\frac{2d}{\pi v} + \tau_- \left(1 - \frac{1}{4} \cos 2\alpha \right) - \right. \quad (1)$$

$$\left. - \tau_+ \sin \alpha + \cos 2\phi \left(\frac{\tau_-}{2} - \tau_+ \sin \alpha + \frac{d}{\pi v} \right) + \tau_+ \sin 2\phi \cos \alpha \right]$$

and

$$(\Delta E)_2 = \frac{e^2 B_0^2 a^2 c B}{2 \pi d m \gamma} \left[\frac{2d}{\pi v} + \tau_- \left(1 - \frac{1}{2} \cos 2\alpha \right) - \right. \quad (2)$$

$$\left. - \tau_+ \sin \alpha + \cos 2\phi \left(-\tau_+ \sin \alpha \right) + \tau_+ \sin 2\phi \cos \alpha \right].$$

τ_+ , τ_- and α are given by

$$\tau_{\pm} = \frac{1}{\omega - \pi v/d} \pm \frac{1}{\omega + \pi v/d}, \quad \alpha = \frac{\omega d}{2v}.$$

B_0 is the amplitude of the z-component of the magnetic field which is zero at $x = a/2$. ϕ is an arbitrary phase.

Energy gain values obtained by the perturbing object method

By means of the perturbing object technique the fields in the plane $x = a/2$ of the cavity shown in fig. 1 with the dimensions $a = 0.10$, $b = 0.486$, $d = 0.208$ m and the resonance frequency $\nu_R = 1.533$ GHz were measured. Two drift tubes with apertures of 25 cm and 4 cm in y- and x-directions, respectively, were used. The drift tubes were of rectangular and pointed shape with an angle of 120° at the top (cf. fig. 1, full and dotted lines). The cavity fields are perturbed by the drift tubes resulting in an E_z -component to be different from zero away from the axis. Fig. 2 shows the field distributions 1 cm off the axis with the straight and the pointed tube inserted, respectively. The main difference between the two field distributions is that the E_y -component for the straight drift tube is much smaller than for the pointed one. Because of the small E_y -component the accelerating effect with two orthogonal E - and B -fields having a phase difference of $\pi/2$ does not work. Instead, the E_y -component causes together with the E_z -component another accelerating effect which is reversed in sign. This effect depends strongly on the y-component of the gradient of E_z which can be deduced from fig. 3. The effect decreases with the gradient of E_z being zero at $|y - b/2| \approx 6$ cm. For larger values of $|y - b/2|$ the gradient of E_z and the accelerating effect caused by E_y and E_z change sign. The sign of the effect for all y-values is reversed by mounting the drift tube at the rear plate of the resonator. For the pointed drift tube the $[E \times B]$ -effect works. For large $|y - b/2|$ -values

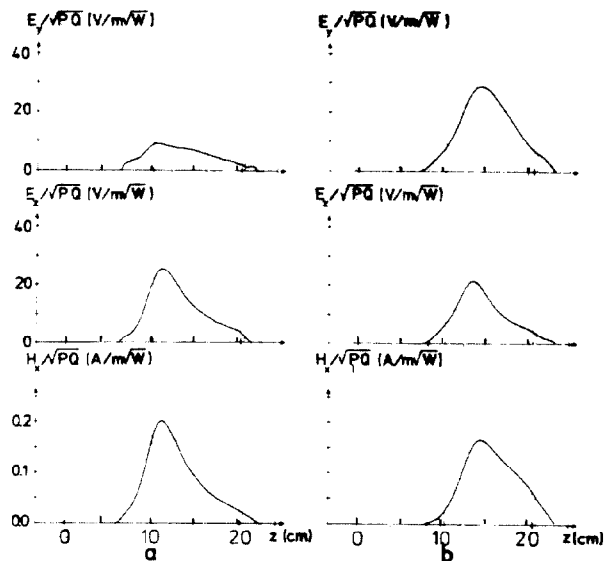


Fig.2. Results of perturbing object measurements of electric and magnetic field components within the plane $x = a/2$ at $y = b/2 + 1$ cm. P_1 is the power loss, Q the Q-factor. The full lines represent smoothed curves which were obtained by cubic spline functions. The distance between the measured points is 0.175 cm. a. Rectangular drift tube. b. Pointed drift tube.

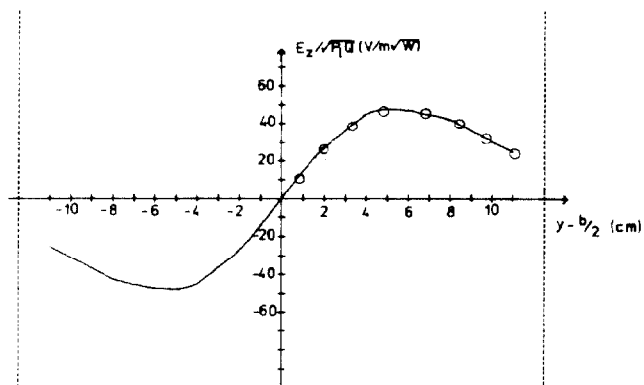


Fig.3. E_z -component versus the y -coordinate at $z = 16.3$ cm for the pointed drift tube. The measured points are marked. The full line results from smoothing cubic spline functions.

the sign of the effect changes, too, because the B_x -field becomes partly negative. The sign of B_x was determined from an independent calculation of B_x from $\vec{B} = -\text{rot } \vec{E}$, thereby using the measured E_y - and E_z -values.

Thus, in both cases energy gains result within a y -range of about 10 cm as can be deduced from fig. 4, where the time averaged energy gain of an accelerating stage $\langle \Delta E \rangle_t$ versus y is plotted for an incident energy of 8.83 MeV.

Energy gain measurements

The energy gain of electrons of 20 keV after having passed one cavity was directly measured by means of a retarding-field analyzer. For this experiment a larger cavity with $a = 0.254$, $b = 0.300$, $d = 0.553$ m, $\nu_R = 0.639$ GHz and drift tubes with circular cross sections were used. The results ΔE versus phase ϕ for a drift tube with 4 cm diameter, an amplitude $B_0 = 1.6$

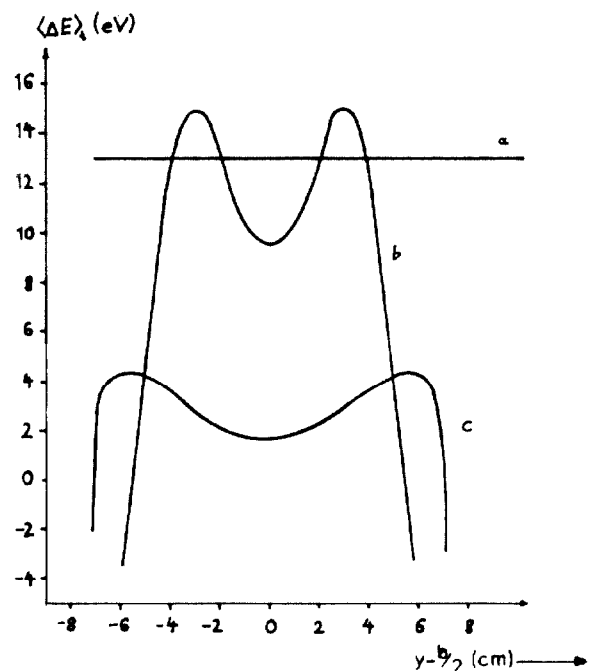


Fig.4. Time-averaged energy gain of electrons of $T = 8.83$ MeV having passed an accelerating stage of four cavities at different distances y from the axis. $P_1 = 200$ W for each cavity. a. Ideal field theory. b. Calculation based on perturbing object data obtained with the rectangular drift tube. It is assumed that the particles pass the cavities in the opposite direction. c. Calculation using pointed drift tube data.

Gauss and a parallel incoming beam at $y = b/2$ are shown in fig. 5. The agreement with values obtained by the perturbing object method³ and even by the ideal field theory (eq. 1) is good. Fig. 6 shows ΔE versus $y - b/2$ for an inclined incident beam of 0.4° , where y is measured at the analyzer diaphragm 54.8 cm behind the drift tube. A 10 cm diameter drift tube was used¹, B_0 being 1.9 Gauss. The measured points agree quite well with the values obtained by the perturbing object method.

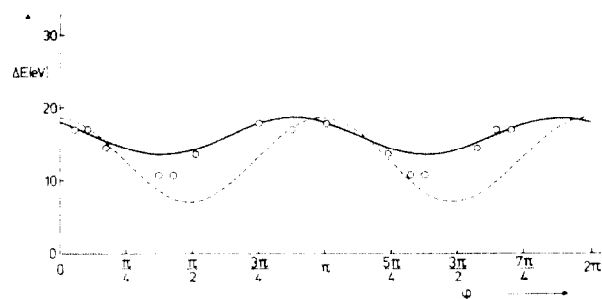


Fig.5. Results of energy gain measurements of electrons after passage of a single cavity. Parallel incoming particles at $y = b/2$. Incident energy 20 keV. Cavity dimensions: $a = 0.254$, $b = 0.300$, $d = 0.553$ m. $B_0 = 1.6$ Gauss. A cylindrical drift tube with 4 cm diameter was used. Full line: Calculation using measured fields. Dashed line: Ideal field theory.

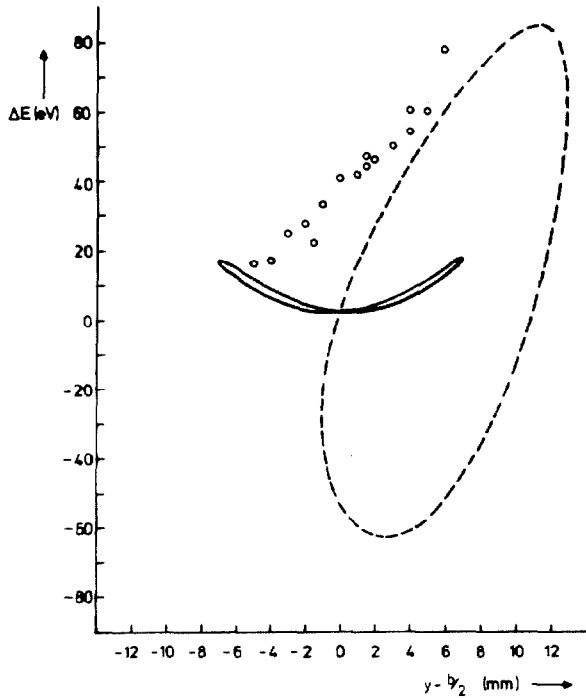


Fig. 6. Results of energy gain measurements versus the deviations $y - b/2$ of the beams at the analyzer 54.8 cm behind the drift tube. $B_0 = 1.9$ Gauss. A cylindrical drift tube with 10 cm diameter was used. The full and dashed lines represent calculations using measured fields for beams coming in at $y = b/2$ parallel to the axis and inclined by 0.4° against the axis, respectively.

Sketch of a phase-free accelerator

In order to accelerate continuous beams of particles phase-free stages must be combined with a circular FFAG guide field. In fig. 7 one period of a spiral ridge magnetic guide field with one cavity is sketched. The guide field is designed to yield the reference orbits between 1 and 51 MeV within a radial range of 25 cm. The largest distance of the 51 MeV orbit from the center is 1.27 m. The radial and axial betatron frequency numbers are 4.67 and 3.79. Cavities with enlarged usable radial ranges are placed within the gaps of the magnets. The result of a numerical calculation of $\langle \Delta E \rangle_t$ for 1 MeV incident energy versus the number n of cavities which were passed is shown in fig. 8. Thereby, the hard edge magnetic guide field and ideal cavity fields were used. The numerically calculated $\langle \Delta E \rangle_t$ -values lie between $n \cdot \langle (\Delta E)_1 \rangle_t$ and $(n/4) \cdot \langle (\Delta E)_2 \rangle_t$. In order to compensate for the energy loss by radiation at 51 MeV an amplitude of the electromagnetic field $B_0 = 4$ Gauss must be maintained in the cavities. The cavity fields perturb the reference orbits radially. In fig. 9 the radial displacements g_{1r} of the reference orbit at 1 MeV related to the radius of curvature $\rho = 0.38$ m and the angular deviations g_{2r} are shown⁴. These deviations might be used for particles injection. With such a device it might be possible to accumulate a high circulating current on the final reference orbit if coherent instabilities can be suppressed. This seems to be possible in our case because of the large momentum spread of the particles on adjacent reference orbits⁵.

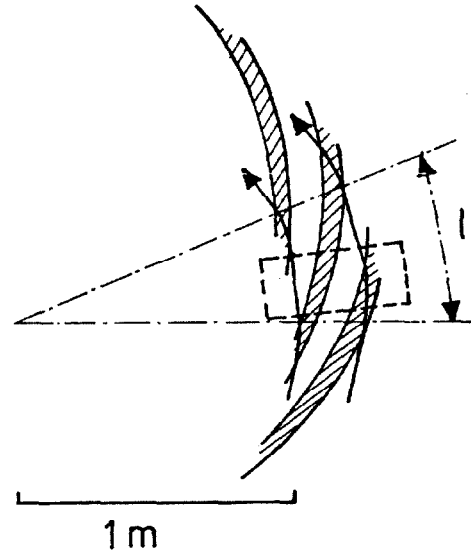


Fig. 7. Spiral ridge FFAG field. A period of length l , a cavity and reference orbits corresponding to 1 and 51 MeV are drawn. The shaded area marks the shape of the magnetic poles. A hard edge model is assumed. The magnetic field increases radially from 124 to 3590 Gauss in the shown range of reference orbits.

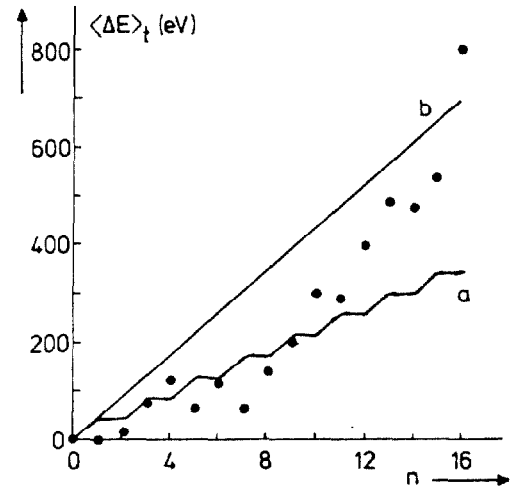


Fig. 8. Numerical calculation of $\langle \Delta E \rangle_t$ versus number n of passed cavities using hard edge guide field and ideal cavity fields. $T = 1$ MeV. $P_1 = 200$ W/cavity. a. $n \cdot \langle (\Delta E)_1 \rangle_t$ vs. n . b. $(n/4) \cdot \langle (\Delta E)_2 \rangle_t$ vs. n .

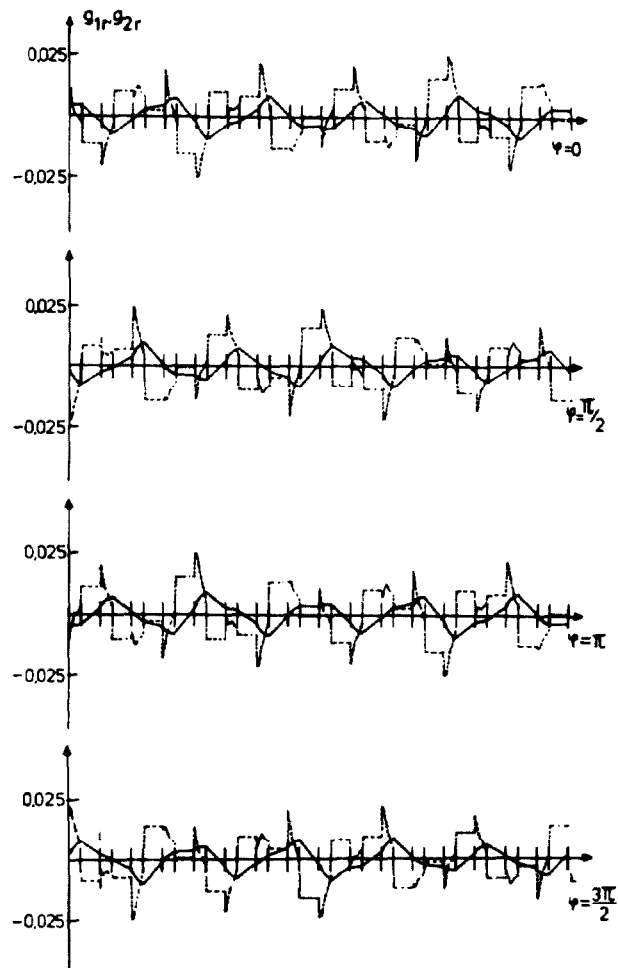


Fig.9. Calculated radial and angular deviations of the 1 MeV reference orbit due to the cavity fields at different phases. $B_0 = 4$ Gauss. The radial deviations g_{1r} are related to the radius of curvature of the circular part of the orbit $\rho = 0.38$ m.

References

1. W. Schott, H.-J. Winter, H. Hagn, K. Springer, H. Zinner, F. Brunner and H. Daniel, 9th Int. Conf. on High Energy Accelerators, Stanford 1974, p. 304.
2. H. Zinner, W. Schott, W. Wilhelm, Nucl. Instr. and Methods, in press.
3. F. Brunner, W. Schott and H. Daniel, IEEE Trans. on Microwave Theory and Techniques, in press.
4. W. Schott, Internal Report, in preparation.
5. C. E. Nielsen, A. M. Sessler and K. R. Symon, Int. Conf. on High Energy Accelerators, CERN, Geneva, 1959, p. 239.